

Exploring Information-Theoretic Metrics

Associated with Neural Collapse in Supervised Training

Kun Song^{1†}, Zhiquan Tan^{2†}, Bochao Zou¹, Jiansheng Chen¹,
Huimin Ma^{1*}, Weiran Huang^{3*}

1 School of Computer and Communication Engineering,
University of Science and Technology Beijing, Beijing, 100083, China.

2 Department of Mathematical Sciences,
Tsinghua University, Beijing, 100084, China.

3 MIFA Lab, Qing Yuan Research Institute, SEIEE,
Shanghai Jiao Tong University, Shanghai, 200240, China.

*Corresponding author(s). E-mail(s): mhmpub@ustb.edu.cn;
weirang.huang@outlook.com;

Contributing authors: songkun@xs.ustb.edu.cn;
tanzq21@mails.tsinghua.edu.cn; zoubochao@ustb.edu.cn;
jschen@ustb.edu.cn;

† These authors contributed equally to this work.

Abstract

In this paper, we utilize information-theoretic metrics like matrix entropy and mutual information to analyze supervised learning. We explore the information content of data representations and classification head weights and their information interplay during supervised training. Experiments show that matrix entropy cannot solely describe the interaction of the information content of data representation and classification head weights but it can effectively reflect the similarity and clustering behavior of the data. Inspired by this, we propose a cross-modal alignment loss to improve the alignment between the representations of the same class from different modalities. Moreover, in order to assess the interaction of the information content of data representation and classification head weights more accurately, we utilize new metrics like matrix mutual information ratio (MIR) and matrix information entropy difference ratio (HDR). Through theory and experiment, we show that HDR and MIR can not only effectively describe the information interplay of supervised training but also improve the performance of supervised and semi-supervised learning.

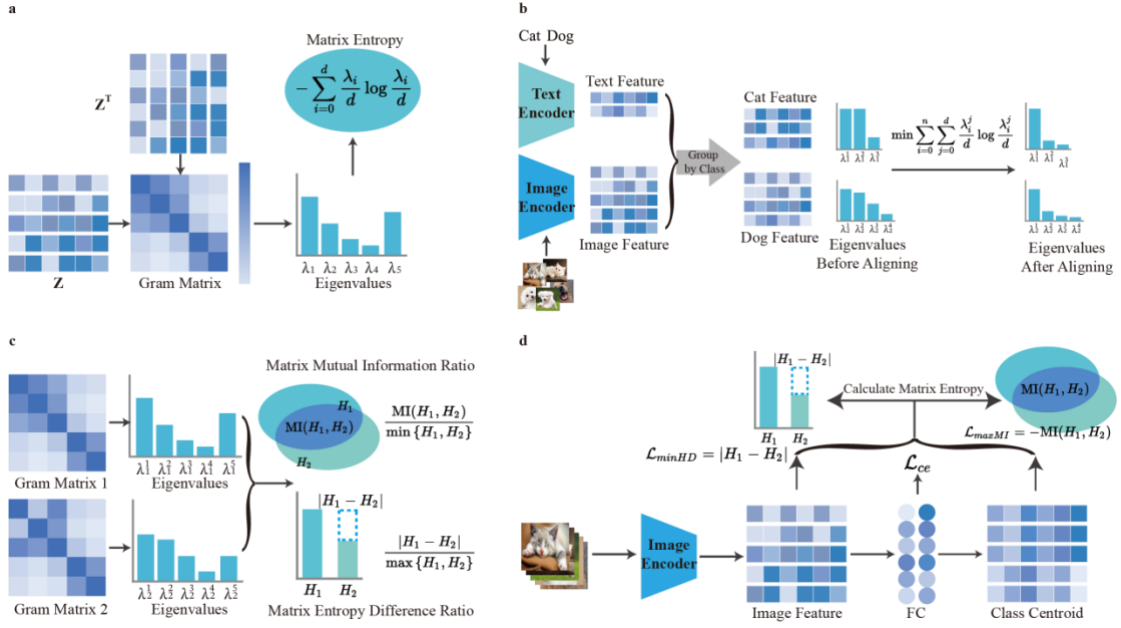


Fig. 1: The overview of our paper. **a, The calculation of matrix entropy.** First, calculate the gram matrix of a set of representations. Then calculate the eigenvalues of the gram matrix. Finally, calculate matrix entropy based on normalized eigenvalues and the definition of Shannon entropy. **b, Align domain features with cross-modal alignment loss.** First, extract the image features and text features. Then, group features by class. Finally, calculate the matrix entropy of each class and minimize the sum of matrix entropy. **c, The calculation of matrix mutual information ratio (MIR) and matrix entropy difference ratio (HDR) between two set of representations.** First, calculate the eigenvalues of the gram matrices generated by two sets of representations respectively. Then calculate the mutual information and matrix entropy difference between the two matrices generated by these two groups of representations. **d, Optimize supervised training with matrix mutual information and matrix entropy difference.** First, extract the feature of a batch of data. On the one hand, input the feature into fully connected layer and calculate the cross-entropy loss, on the other hand, regard the classification weight of each class as the class center and collect the class centroid of each data according to the labels. Then, maximize the MIR and minimize the HDR of the two Gram matrices generated by data feature and class centroids.

Supervised learning is a significant part of machine learning, tracing its development back to the early days of artificial intelligence. Leveraging ample annotated data from large-scale datasets like ImageNet¹ and COCO², supervised learning has achieved outstanding performance in tasks such as image recognition, natural language processing, and speech recognition. These advancements have significantly propelled the field of artificial intelligence forward. Concurrently, with its enhanced performance in real-world applications, some interesting phenomena in supervised learning, such as Neural Collapse³, linear mode connectivity⁴, and grokking⁵ have emerged. An increasing amount of research is exploring the reasons behind these phenomena.

Neural Collapse³ (NC) is an interesting phenomenon observed during the training process of supervised learning. In different stages of network training, data

representation within the same class become more and more similar in the feature space, meaning that intra-class differences decrease. At the same time, data representation of different classes become more distinct in feature space, leading to more significant inter-class differences. In supervised learning classification tasks, after prolonged training, an alignment has emerged between the weight of the final fully connectivity layer and the corresponding representations of class centroids. This indicates that for each class, the centroid of its representations almost coincides with the weight vector of its corresponding classifier.

Existing research on Neural Collapse primarily focuses on the similarity between data representations and classification head weights. In this paper, we provide new theoretical insights for Neural Collapse from the perspective of information theory. Considering that Shannon entropy need to estimate the distribution of representations, we utilize matrix entropy as an analytical tool to describe the information contents accurately ([Fig.1 a](#)). Firstly, theoretical analysis of the matrix entropy of data representations and classification head weights when Neural Collapse occurs is provided. Observations throughout the training process show that the variation of the matrix entropy meets the theoretical derivations. Additionally, under different temperature coefficients in the softmax function, we find an interesting phenomenon: the matrix entropy tends to decrease as the temperature increases. Based on this, we discover a correlation between the matrix entropy of a set of data representations and the clustering properties of those data representations. Considering the similarity between clustering and cross-modal alignment, we propose a novel cross-model alignment loss (CMA) to optimize the supervised fine-tuning of pre-trained models by aligning knowledge across different modalities ([Fig.1 b](#)). Experiments demonstrate that although the matrix information entropy of data representations cannot directly determine the state of neural collapse, it can serve as a regularization term to assist in optimizing knowledge alignment during the supervised fine-tuning of cross-modal pre-trained models.

To further describe the detailed information interplay in supervised learning, we propose two new metrics, the Matrix Mutual Information ratio (MIR) and the Matrix Entropy Difference Ratio (HDR)⁶ ([Fig.1 c](#)). When Neural Collapse occurs, there is excellent alignment between data representations and classification head weights, resulting in identical matrix entropy. Theoretical analysis provides the values of MIR and HDR under conditions of neural collapse. Observations indicate that MIR and HDR between data representations and classification head weights approach to the theoretical value, which prove the effective of MIR and HDR. Moreover, our research also suggests that MIR and HDR can describe the other phenomena in supervised learning such as Linear Mode Connectivity and Grokking. Meanwhile, information interplay can be introduced into supervised learning as extra loss terms to optimize the learning process ([Fig.1 d](#)). Experiment demonstrates that MIR and HDR can not only assess Neural Collapse but also improve model performance as regularization terms.

Problem setup

Supervised learning problem

Given a labeled dataset $\{(x_i, y_i)\}_{i=1}^n$, where $y_i \in \{1, 2, \dots, C\}$ is the class label. In this paper, we mainly consider training an image classification problem by concatenation of a deep neural network h and a linear classifier. The linear classifier consists of a weight matrix $W \in \mathbb{R}^{C \times d}$ and $b \in \mathbb{R}^{C \times 1}$. Denote $W^T = [w_1 \dots w_C]$. The training loss is the cross-entropy loss, i.e.,

$$\mathcal{H}(p, q) = - \sum_{i=0}^n p(x_i) \log q(x_i),$$

where p is the true probability distribution, and q is the predicted probability distribution.

Meanwhile, we briefly summarize the three most important Neural Collapse³

conditions for our paper. Denote $\mu_G = \frac{\sum_{i=1}^n h(x_i)}{n}$ and $\mu_c = \frac{\sum_{y_i=c} h(x_i)}{\#\{y_i=c\}}$ be the global mean and class-wise mean respectively. Then we define $\tilde{\mu}_c = \mu_c - \mu_G$.

(NC 1) $h(\mathbf{x}_i) = \mu_{y_i}$ ($i = 1, 2, \dots, n$).

(NC 2) $\cos(\tilde{\mu}_i, \tilde{\mu}_j) = \frac{c}{c-1} \delta_j^i - \frac{1}{c-1}$, where $\cos(\cdot)$ is the cosine similarity and δ_j^i is Kronecker symbol.

(NC 3) $\frac{W^T}{|W|_F} = \frac{\mathbf{M}}{|\mathbf{M}|_F}$, where $\mathbf{M} = [\tilde{\mu}_1 \dots \tilde{\mu}_C]$.

Matrix entropy and mutual information

The following definitions of matrix entropy and matrix mutual information are taken from this paper⁷.

Definition 1. (Matrix Entropy) Suppose a positive-definite matrix $\mathbf{K} \in \mathbb{R}^{d \times d}$ which $\mathbf{K}(i, i) = 1$ ($1 \leq i \leq d$). The matrix entropy is defined as follows:

$$H(\mathbf{K}) = -\text{tr} \left(\frac{1}{d} \mathbf{K} \log \frac{1}{d} \mathbf{K} \right) = - \sum_{i=0}^d \frac{\lambda_i}{d} \log \left(\frac{\lambda_i}{d} \right).$$

Definition 2. (Effective Rank⁸) The effective rank of the matrix \mathbf{A} , denote $\text{erank}(\mathbf{A})$, is defined as

$$\text{erank}(\mathbf{A}) = \exp \left(H(p_1, p_2, \dots, p_Q) \right) = \exp \left(- \sum_{k=1}^Q p_k \log(p_k) \right),$$

where $p_i = \frac{\sigma_i}{\sum_{k=1}^n \sigma_k}$, $\{\sigma_i | i = 1, \dots, n\}$ are the singular values of \mathbf{A} .

Definition 3. (Matrix mutual information) The matrix mutual information is defined as follows:

$$\text{MI}(\mathbf{K}_1, \mathbf{K}_2) = H(\mathbf{K}_1) + H(\mathbf{K}_2) - H(\mathbf{K}_1 \odot \mathbf{K}_2),$$

where \odot is the Hardmard product.

In order to calculate the entropy of a set of representation, we introduce a standard way of constructing a gram matrix as follows.

Definition 4. (Construction of gram matrix). Given a set of representations $\mathbf{Z} = [\mathbf{z}_1 \cdots \mathbf{z}_N] \in R^{d \times N}$. Denote the l_2 normalized feature $\hat{\mathbf{z}}_i = \frac{\mathbf{z}_i}{\|\mathbf{z}_i\|}$, $\hat{\mathbf{Z}} = [\hat{\mathbf{z}}_1 \cdots \hat{\mathbf{z}}_N]$. Then gram matrix is defined as $G(\mathbf{Z}) = \hat{\mathbf{Z}}^T \hat{\mathbf{Z}}$.

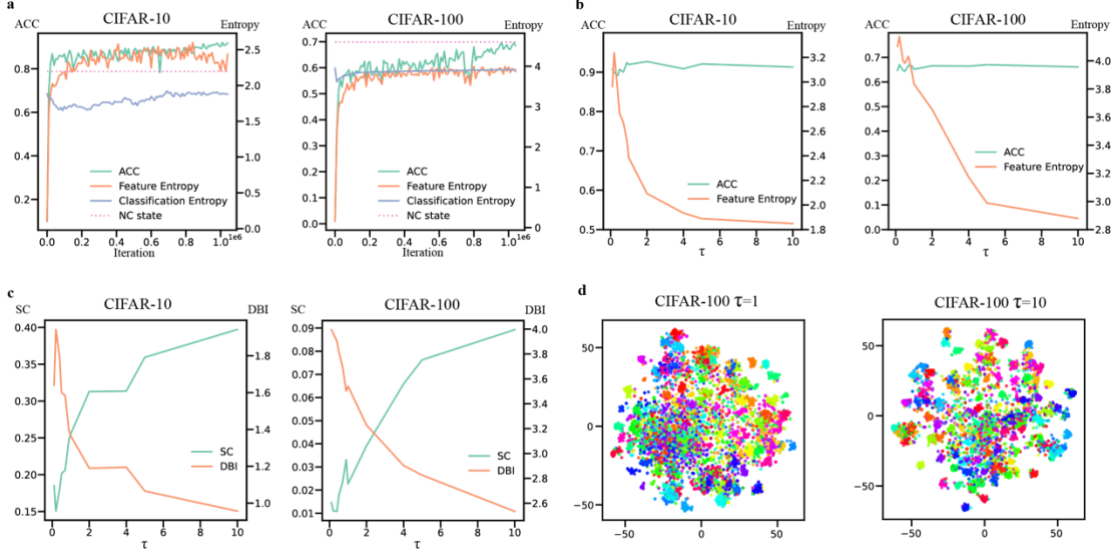


Fig. 2: **a**, The changes in model accuracy, the matrix information entropy of data representations and classification head weights during the model training process on CIFAR-10 and CIFAR-100. **b**, The relationship between accuracy, matrix information entropy of data representations, and the temperature coefficient of softmax. **c**, The SC (Silhouette Coefficient) and DBI (Davies-Bouldin Index) of representation extracted by models trained with different temperature coefficients. **d**, Train models on CIFAR-10 using temperature coefficients of 1 and 10, respectively, and use t-SNE to visualize the test set features. **e**, Train models on CIFAR-100 using temperature coefficients of 1 and 10, respectively, and use t-SNE to visualize the test set features.

Results

Matrix entropy in supervised learning

We theoretically analyze the properties of matrix entropy and provide the theoretical values of matrix entropy for data representation and classifier weights in the case of Neural Collapse.

Theorem 1. Given a set of representations $\mathbf{f} = [h(x_1), h(x_2), \dots, h(x_n)]$, if $H(G(\mathbf{f})) = 0$, the similarities between any representations are 1, i.e., all the representations are the same, $h(x_1) = h(x_2) = \dots = h(x_n)$.

Theorem 2. Suppose Neural Collapse happens, $\text{erank}(G(\mathbf{M})) = C - 1$. If the dataset is class-balance, for all representations $f = [h(x_1), h(x_2), \dots, h(x_n)]$ in datasets, $H(G(f)) = H(G(W^T)) = H(G(\mathbf{M})) = \log(C - 1)$.

Matrix entropy during standard supervised training. As shown in [Fig. 1 a](#), we utilize matrix entropy to measure the information content of a set of features. According to [Theorem 2](#), the entropy of data representations and classification is related to the number of categories under the Neural Collapse state. As shown in [Fig. 2 a](#), we observe that the matrix entropy of the data representation is close to zero at the beginning of training. This is because the similarity among data representation in the dataset is high, meaning that the initial data representations cannot distinguish samples among different classes. As training progresses, the matrix entropy of the data representations increases, indicating that the discrimination among samples increases, and the model's accuracy improves simultaneously. What's more, compared to the matrix entropy of the data representation, the matrix information entropy of the classifier head weights is close to the Neural Collapse state at the initial stage. This occurs because the randomly initialized classifier head weights differ significantly, resulting in an initial Gram matrix that is nearly an identity matrix. However, at this point, the classifier head does not contain any class information, resulting in very low classification performance. After the first few epochs of initial training, the matrix entropy of the classifier head weights decreases rapidly. This indicates that after a few epochs of training, the classifier head can simply distinguish different classes. As training continues, the matrix entropy of the classification head weights continues to increase, enhancing the classifier head's ability to discriminate between different class information.

However, at the end of training, the entropy of data representations and classification head weights trained on CIFAR-10 and CIFAR-100 do not reach the Neural Collapse state (i.e., entropy of the data representation and classification head weights for CIFAR-10 is $\ln 9$ and for CIFAR-100, it is $\ln 99$). On CIFAR-10, although the data representations reach the Neural Collapse state during training, the entropy of these representations continued to increase, due to the weights of the classification head not yet reach the Neural Collapse state. On CIFAR-100, neither the entropy of the data representations nor the classification head reaches the NC state by the end of training.

In summary, we can derive the theoretical values of information entropy for data representation and classifier head weights under the NC state. However, due to the inconsistent training progress between the feature extractor and the classifier head, relying solely on the entropy of data representation or classifier weights is insufficient to determine whether the model has reached the Neural Collapse state.

Matrix entropy in softmax. Softmax is used in machine learning to convert representations into probability distribution, with the temperature coefficient often controlling the smoothness of this distribution. [Fig. 2 b](#) illustrates the accuracy and

the information entropy of the data representation for models trained with different temperature coefficients. Although the accuracy varies little across different temperatures, the information entropy of the data representation matrix decreases significantly with increasing temperature. According to [Theorem 1](#), lower information entropy of data representations indicates higher similarity among these representations, resulting in better clustering performance.

To better quantify the clustering effect of representations, we use Silhouette Coefficient¹⁰ and Davies-Bouldin Index¹¹ to measure the clustering properties of the representations.

Silhouette Coefficient, $S(i) = \frac{b(i)-a(i)}{\max(a(i),b(i))}$, is a measure of how similar a sample is to its own class center compared to other classes, where $a(i)$ is the average distance between a sample and all other points in the same cluster and $b(i)$ is the average distance between a sample and all points in the next nearest cluster. Davies-Bouldin Index is based on a ratio of within-cluster scatter to between-cluster separation, providing an intuitive measure of cluster compactness and

separation. $R_{ij} = \frac{S_i+S_j}{M_{ij}}$, where S_i is the average distance between each point in the cluster and the centroid of the cluster and M_{ij} is the distance between the centroids of clusters i and j . As shown in [Fig. 2 c](#), Silhouette Coefficient of the features extracted by the model trained with a higher temperature coefficient is higher, and Davies-Bouldin Index is lower. Compared with [Fig.2 b](#), it can be seen that lower information entropy means better clustering of the features. We also visualize the features extracted by the models trained with temperature coefficients of 1 and 10. As shown in [Fig. 2 d](#), compared to the model trained with temperature coefficient of 1, the features extracted by the model with a temperature coefficient of 10 are more compact within the same class and have more significant distances between classes.

According to [Theorem 1](#) and [Fig. 2 b c d](#), it can be concluded that for a set of data, lower matrix information entropy implies better clustering performance.

Cross-Modal Alignment loss improve cross modal few-shot fine-tuning.

Considering the relationship between matrix information entropy and representation clustering performance, we propose to use matrix information entropy to align the feature across different feature. As shown in [Fig. 1 b](#), we proposed a Cross-Modal Alignment loss (CMA). Specially, representations from different modalities are grouped by category, and we calculate sum of the matrix entropy of these matrices. In order to assess the effectiveness, we fine-tune CLIP¹² in few-shot setting. As shown in [TABLE 1](#), the results indicate that CMA outperforms CoOp¹³ in terms of average performance across 11 datasets. In most datasets, CMA significantly improves the performance of CoOp. These results demonstrate that CMA can align features of different modalities well by optimizing the matrix entropy of features for different modalities within the same category separately.

TABLE 1: Results of fine-tuning CLIP with cross-modal alignment (CMA) loss. All results are trained from three runs and calculated with 95% CI. We followed the setup of CoOp, fine-tuning CLIP under three different random seeds and calculating the average. The results for ID (in distribution) are the performance of CLIP with few-shot fine-tuning on different datasets. The results of base to novel are obtained by performing 16-shot fine-tuning of CLIP on the base and testing on the novel classes. The performance is under different weight of CMA and cross-entropy loss. Value 0 indicates fine-tuning the model using only cross-entropy loss, while 1 represents fine-tuning the model using only CMA loss. Finally, we measured the impact of using CMA on cross-modal similarity. ‘‘Class Similarity’’ represents the similarity between image representations and the corresponding class’s text representations. ‘‘Modal Similarity’’ represents the average similarity between any image representation and the text representations of all categories.

In Distribution											
Method	ZS	CoOp w/o CMA					CoOp w/ CMA				
Shot Num	0	1	2	4	8	16	1	2	4	8	16
Caltech101 ¹⁴	86.29	87.90 \pm 0.56	87.70 \pm 1.63	89.33 \pm 0.14	90.03 \pm 0.66	91.00 \pm 0.51	87.80 \pm 1.25	88.43\pm1.28	89.33\pm0.14	89.97\pm0.47	91.53\pm0.14
DTD ¹⁵	42.32	45.13 \pm 1.52	47.40 \pm 1.44	53.63 \pm 0.96	58.90 \pm 0.73	63.20 \pm 0.58	44.60 \pm 1.62	47.47\pm1.73	53.83\pm0.51	60.37\pm1.08	63.90\pm1.03
EuroSAT ¹⁶	37.56	52.77 \pm 5.62	59.47 \pm 5.71	70.03 \pm 2.83	77.73 \pm 1.17	83.83 \pm 1.35	51.57 \pm 3.78	59.43 \pm 2.47	70.10\pm1.60	77.30 \pm 2.48	83.80 \pm 1.04
Aircraft ¹⁷	17.28	8.03 \pm 6.5	17.57 \pm 3.02	21.13 \pm 2.06	26.67 \pm 0.93	31.63 \pm 0.88	13.73\pm4.35	18.30\pm3.12	21.60\pm1.22	25.87 \pm 0.38	29.30 \pm 0.09
Food101 ¹⁸	77.31	74.17 \pm 1.59	71.40 \pm 1.58	73.37 \pm 3.51	71.80 \pm 0.70	74.50 \pm 0.00	76.23\pm0.63	74.17\pm1.10	75.37\pm2.36	72.70\pm1.21	75.50\pm0.24
ImageNet ¹	58.18	55.73 \pm 0.77	55.93 \pm 0.23	58.43 \pm 0.32	60.43 \pm 0.05	60.87 \pm 0.47	55.77\pm1.15	56.57\pm0.70	58.17 \pm 0.23	59.87 \pm 0.11	60.33 \pm 0.79
Flowers ¹⁹	66.14	68.73 \pm 2.88	77.20 \pm 2.00	85.27 \pm 2.27	91.53 \pm 0.72	94.63 \pm 0.28	67.10 \pm 1.45	78.57\pm1.73	85.50 \pm 0.64	91.37 \pm 0.88	94.13 \pm 0.19
OxfordPets ²⁰	85.77	86.27 \pm 0.75	82.10 \pm 1.47	86.97 \pm 0.90	85.67 \pm 0.51	86.37 \pm 0.42	87.07\pm0.38	86.77\pm1.40	88.43\pm0.23	87.03\pm1.35	88.50\pm0.70
Cars ²¹	55.61	55.47 \pm 1.90	58.30 \pm 0.83	62.50 \pm 0.18	67.90 \pm 0.55	73.07 \pm 0.42	55.23 \pm 2.54	58.73\pm0.53	62.80\pm0.18	68.03\pm0.11	73.03 \pm 0.65
SUN397 ²²	58.52	60.20 \pm 0.37	59.77 \pm 0.93	62.73 \pm 0.91	65.17 \pm 0.05	68.87 \pm 0.11	59.77 \pm 1.03	59.50 \pm 0.61	62.73\pm0.19	65.23\pm0.71	68.60 \pm 0.4
UCF101 ²³	61.46	61.90 \pm 0.72	64.30 \pm 1.44	67.57 \pm 1.24	73.07 \pm 0.32	75.80 \pm 0.74	63.90 \pm 1.39	65.10\pm0.51	68.40\pm0.51	72.37 \pm 1.23	75.93\pm0.38
Average	58.77	59.66	61.92	66.45	69.90	73.07	60.22	63.00	66.93	70.01	73.20

Base to Novel											
Weight	0	0.1	0.2	0.3	0.4	0.5	0.6	0.7	0.8	0.9	1
EuroSAT ¹⁶	53.10 \pm 18.43	49.43 \pm 12.52	61.13 \pm 1.52	51.40 \pm 21.86	66.27 \pm 2.52	58.17 \pm 9.00	55.87 \pm 7.10	64.5 \pm 8.14	67.97\pm13.80	53.13 \pm 2.92	49.37 \pm 4.47
OxfordPets ²⁰	91.93 \pm 0.97	93.37 \pm 6.63	97.63 \pm 0.11	97.03 \pm 1.01	97.77\pm0.47	96.63 \pm 0.92	97.30 \pm 0.37	97.50 \pm 0.37	95.77 \pm 1.74	89.07 \pm 2.36	78.07 \pm 5.17
DTD ¹⁵	48.33 \pm 5.14	50.23 \pm 2.88	51.67 \pm 4.79	52.93\pm0.84	50.83 \pm 4.19	50.07 \pm 3.52	48.87 \pm 3.79	54.50 \pm 4.26	50.10 \pm 1.71	51.10 \pm 0.61	37.50 \pm 3.10
Aircraft ¹⁷	21.2 \pm 15.55	31.37\pm1.04	22.87 \pm 1.41	16.23 \pm 11.11	19.93 \pm 6.02	23.10 \pm 13.05	23.00 \pm 9.81	19.23 \pm 10.26	28.33 \pm 1.01	24.57 \pm 1.63	19.53 \pm 0.99
Caltech101 ¹⁴	93.20 \pm 0.53	93.37 \pm 0.47	94.23\pm0.71	93.90 \pm 0.80	93.70 \pm 0.00	93.30 \pm 0.24	93.03 \pm 0.54	93.07 \pm 0.14	93.40 \pm 1.20	90.70 \pm 1.11	86.93 \pm 2.13
UCF101 ²³	73.23 \pm 2.51	69.37 \pm 3.73	73.77 \pm 4.58	74.00 \pm 2.24	73.90 \pm 1.95	75.10\pm3.24	73.00 \pm 2.99	72.33 \pm 4.61	68.53 \pm 0.60	63.17 \pm 0.86	54.53 \pm 5.68
Food101 ¹⁸	91.33 \pm 0.32	91.33 \pm 0.21	91.23 \pm 0.63	91.57\pm0.21	91.23 \pm 0.47	91.27 \pm 0.69	90.50 \pm 0.74	90.60 \pm 0.96	89.87 \pm 0.19	83.60 \pm 3.05	79.63 \pm 0.98
Flowers ¹⁹	70.90 \pm 2.88	67.67 \pm 6.08	73.43 \pm 0.84	72.97 \pm 1.30	73.90\pm1.69	73.53 \pm 3.41	72.47 \pm 0.67	70.20 \pm 1.58	65.67 \pm 2.38	55.20 \pm 3.99	55.87 \pm 3.98
Cars ²¹	72.57 \pm 1.53	72.27 \pm 1.32	72.27 \pm 0.77	72.90 \pm 0.79	73.57\pm1.00	72.97 \pm 1.03	71.30 \pm 0.79	71.43 \pm 0.30	69.60 \pm 1.48	63.97 \pm 1.35	61.33 \pm 0.60
SUN397 ²²	75.97 \pm 0.37	76.13 \pm 0.37	76.60\pm0.88	76.40 \pm 0.00	75.27 \pm 0.28	75.77 \pm 0.86	74.90 \pm 0.81	75.07 \pm 0.38	69.80 \pm 1.43	65.67 \pm 1.11	61.53 \pm 2.65
ImageNet ¹	69.87\pm0.46	69.70 \pm 0.4	69.63 \pm 0.38	69.80 \pm 0.65	69.70 \pm 0.42	69.77 \pm 0.28	69.73 \pm 0.70	67.80 \pm 0.94	62.93 \pm 0.05	58.70 \pm 0.56	50.70 \pm 0.96

	w/o CMA	w/ CMA
Class Similarity	0.318	0.354
Modal Similarity	0.173	0.203

We also compare the impact of CMA on model generalization, we evaluate the base-to-new performance following CoCoOp²⁴. Specifically, the datasets are divided into base classes and novel classes. The model is trained on the base classes (16-shots), and the performance is evaluated on the novel classes. We explored the impact of different weights of CMA loss and cross-entropy loss on model performance. As shown in [TABLE 1](#), performance is improved across most datasets with different CMA weight, indicating the stability of using CMA. For datasets with fewer categories, such as EuroSAT¹⁶, the optimal weight is relatively high, and the performance when fine-tuning using only the CMA loss is higher than when using only the cross-entropy loss. For most datasets, the optimal weights are around 0.3-0.5. However, when the number of classes is sufficiently large, such as with ImageNet¹, CMA does not provide any additional performance improvement. We analyze this phenomenon and conclude that when the number of categories is small, aligning the features of different modalities within the same category does not significantly affect the features of other categories, thereby improving model performance. However, when the number of categories is too large, excessively aligning features across modalities may weaken the model’s inherent modality alignment capability.

In order to further demonstrate the effectiveness of CMA in aligning representations from different modalities, we calculated the similarity of features from different modalities within the same category and the similarity between all data representations across different modalities. As shown in [TABLE 1](#), compared with CoCoOp, CMA can better align the representations of different modalities.

Information interplay in supervised learning

As shown in [Fig.2 a](#), since matrix entropy is not fully accurate in determining whether the model has reached the Neural Collapse state, we propose two new metrics ([Fig.1 c](#)) based on the definition of Neural Collapse as follows:

Definition 5. (Matrix mutual information ratio (MIR)) The matrix mutual information ratio is defined as follows:

$$\text{MIR}(\mathbf{K}_1, \mathbf{K}_2) = \frac{\text{MI}(\mathbf{K}_1, \mathbf{K}_2)}{\min\{H(\mathbf{K}_1), H(\mathbf{K}_2)\}}$$

Definition 6. (Matrix entropy difference ratio (HDR)) The matrix entropy difference ratio is defined as follows:

$$\text{HDR}(\mathbf{K}_1, \mathbf{K}_2) = \frac{|H(\mathbf{K}_1) - H(\mathbf{K}_2)|}{\max\{H(\mathbf{K}_1), H(\mathbf{K}_2)\}}$$

In addition, we provide the theoretical values of the matrix mutual information ratio and the matrix entropy difference ratio among data representations, class centroids, and classification head weights when Neural Collapse occurs.

Theorem 3. Suppose Neural Collapse happens. Then $\text{HDR}(G(W^T), G(\mathbf{M})) = 0$ and

$$\text{MIR}(G(W^T), G(\mathbf{M})) = \frac{1}{c-1} + \frac{(c-2)\log(c-2)}{(c-1)\log(c-1)}.$$

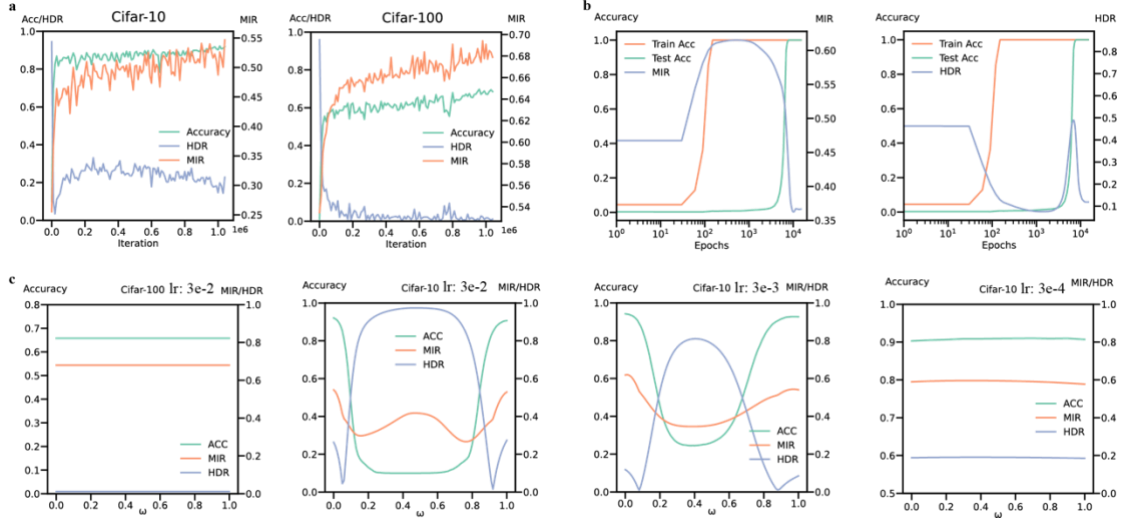


Fig. 3: **a**, The change of accuracy, HDR and MIR between data representations and the classification head weights during the training process. **b**, The change of accuracy on train set, test set and HDR, MIR between data representations and the classification head weights during the grokking process. **c**, Train two models on CIFAR-100 and CIFAR-10 using different initial values with a learning rate of 0.03, and interpolate between them to create a new model. Analyze the relationship between the new model's accuracy, HDR (High-Dimensional Representation), MIR (Mutual Information Rate), and the interpolation weights. In addition, train models on CIFAR-10 using different learning rates ($3e^{-3}$, $3e^{-4}$) and explore the impact of these learning rates on model interpolation.

As the linear weight matrix W can be seen as prototype embedding for each class. It is natural to consider the mutual information and entropy difference between sample embedding and label embedding.

Theorem 4. Suppose the dataset is class-balanced, $\mu_G = 0$ and Neural Collapse happens. Denote $Z_1 = [h(x_1) \cdots h(x_n)] \in \mathbb{R}^{d \times n}$ and $Z_2 = [w_{y_1} \cdots w_{y_n}] \in \mathbb{R}^{d \times n}$.

$$\text{Then } \text{HDR}(Z_1, Z_2) = 0 \text{ and } \text{MIR}(Z_1, Z_2) = \frac{1}{C-1} + \frac{(C-2)\log(C-2)}{(C-1)\log(C-1)}.$$

Information interplay during standard supervised learning process. According to Neural Collapse, during the terminal stages of training, data representations align with the classification head weights. During the training process, MIR increases to its theoretical upper limit, while HDR decreases to 0. We plot the model's accuracy on the test set during the training process, as well as the MIR and the HDR between data representations and the corresponding classification heads. As shown in [Fig.3 a](#), on CIFAR-10 and CIFAR-100, the accuracy and MIR exhibit almost identical trends of variations. In most cases, both accuracy and MIR increase or decrease simultaneously, and MIR consistently shows an upward trend, having its trajectory toward its theoretical maximum value. Contrarily, in most instances, accuracy and HDR show opposite trends, with HDR continually decreasing and even nearing its theoretical minimum value of zero on CIFAR-100. In summary, MIR and HDR effectively describe the process of training towards Neural Collapse.

Information interplay in grokking. In supervised learning, training models on certain datasets can result in an anomalous situation. Initially, models quickly learn the patterns of the training set, but at this point, their performance on the test set is very poor. As training continues, the models learn representations that can generalize to the test set, a phenomenon referred to as Grokking²⁵. We aim to explore the information interplay in Grokking.

As shown in [Fig.3 b](#), we plot the accuracy of both the training and test sets during the grokking process, as well as the variation in MIR and HDR between the representation and the classification head weights. It can be observed that, in the early stages of training, the model quickly fits the training data and achieves 100% accuracy on the training set. However, at this point, the performance on the test set is nearly equivalent to that of random guessing. As training continues, the model gradually shows generalization capability on the test set, ultimately achieving 100% accuracy, which is a hallmark of grokking. [Fig.3 b](#) also reveals a clear two-phase variation in both MIR and HDR between data representation and classification head weights. Initially, similar to fully supervised learning, MIR increases, while HDR decreases. However, as training proceeds, MIR begins to decrease, and HDR starts to increase, indicating the model is seeking new optimal points. After the model achieves the grokking, MIR reaches its lowest, and HDR rapidly declines from its highest point. The experiments demonstrate that HDR and MIR exhibit distinct phenomena in two stages, suggesting that information metrics can describe the grokking phenomenon, providing a basis for further research.

Information interplay in linear mode connectivity. Linear mode connectivity⁴ suggests that under specific datasets and experimental setups, models initialized with the same random parameters will be optimized near the same local optimal basin, even if the order of training data and data augmentation differs. We investigate the behaviors of MIR and HDR under the setting of linear mode connectivity. We initialize models with the same random parameters and train them using different data sequences and random augmentations. Subsequently, we linearly interpolate these two checkpoints and obtain a new model $h = (1 - \omega) \cdot h_1 + \omega \cdot h_2$, where h_1 and h_2 are the two checkpoints and ω is the interpolation weight. Then we test these models on a test set for accuracy, MIR, and HDR.

As shown in [Fig. 3 c](#). On CIFAR-100, the performance of models obtained along the interpolation line is close, aligning with the linear mode connectivity. At this point, MIR and HDR remain almost unchanged. However, on CIFAR-10, the models do not exhibit linear mode connectivity. When the value of interpolation weight is between 0.4 and 0.6, the performance of the interpolated models even drops to that of random guessing. Surprisingly, at this time, MIR shows an additional upward trend. Moreover, when the value of interpolation weight is close to 0 and 1, despite a slight decrease in performance, HDR also decreases. Although we find it difficult to explain this anomaly, it does demonstrate that HDR and MIR have distinctive attributes compared to the accuracy metric, presenting an intriguing avenue for further exploration.

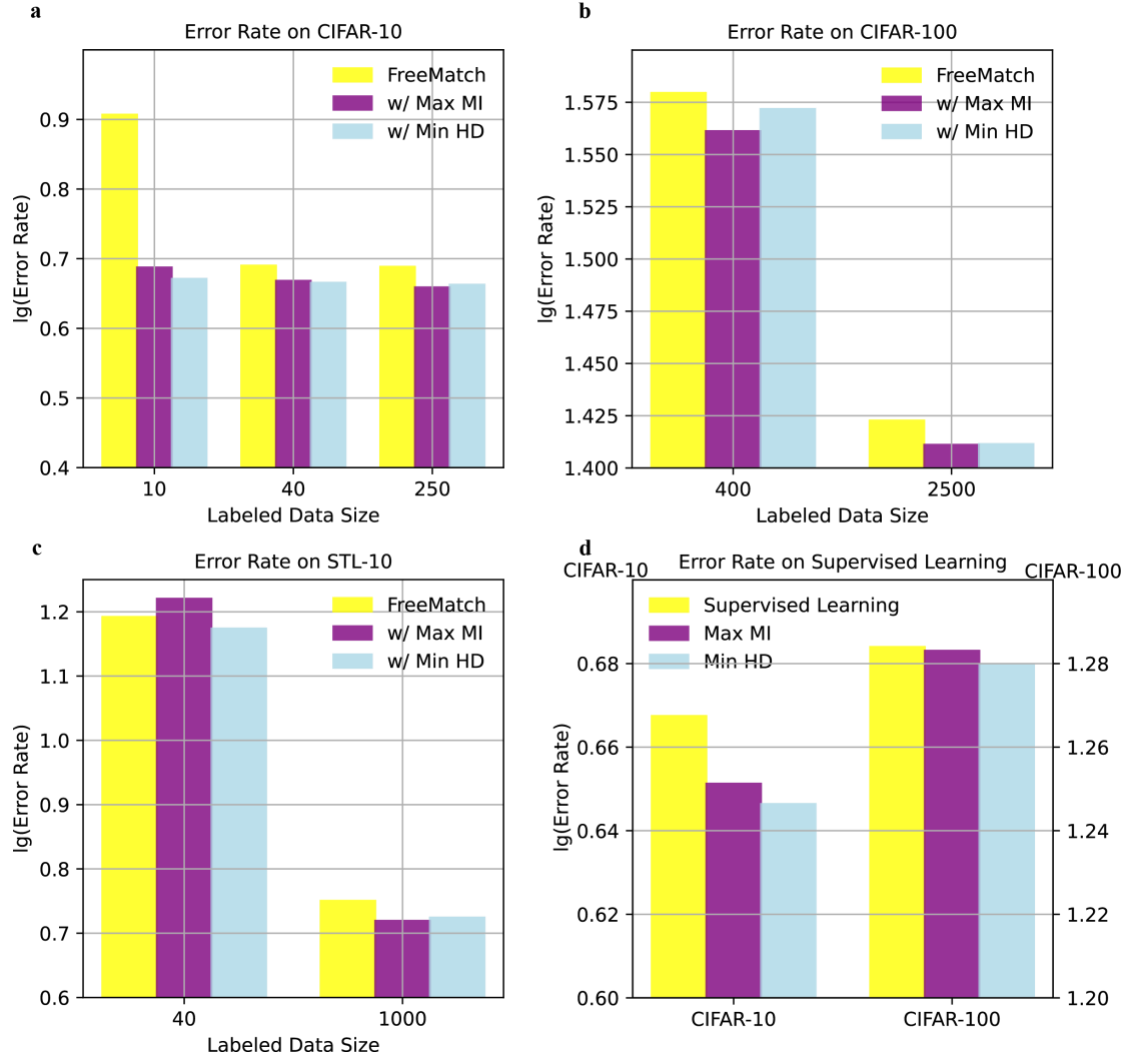


Fig. 4: $\lg(\text{Error rates})$, ($\lg(100\% - \text{accuracy})$) on CIFAR-10/100, and STL-10 datasets for state-of-the-art methods in supervised learning and semi-supervised learning. **a**, $\lg(\text{Error Rates})$ on CIFAR-10 in semi-supervised learning. **b**, $\lg(\text{Error Rates})$ on CIFAR-100 in semi-supervised learning. **c**, $\lg(\text{Error Rates})$ on STL-10 in semi-supervised learning. **d**, $\lg(\text{Error Rates})$ on CIFAR-10 and CIFAR-100 in supervised learning.

Considering that linear mode connectivity is related to the experimental configuration²⁶, we posit that the performance decline of the interpolated model on CIFAR-10 is associated with an excessively high learning rate. In the training phase, models navigate the loss landscapes in search of minimal values, and two models with linear mode connectivity are optimized near the same local optimum. When the learning rate is too high, different training sample ordering and data augmentations lead to directing model optimization towards distinct regions within the loss landscapes. We experiment with different learning rates on CIFAR-10 and test their linear mode connectivity. It is observed that as the learning rate decreased, fluctuations in accuracy, MIR, and HDR also reduced. When the learning rate is lowered to $3e^{-4}$, the model demonstrates linear mode connectivity on CIFAR-10.

This suggests that HDR and MIR are also effective in describing linear mode connectivity when it exists.

MIR and HDR improve supervised learning and semi-supervised learning

Considering that MIR and HDR can effectively describe supervised learning, we apply them into supervised learning and semi-supervised learning. As shown in [Fig.1 d](#), we train supervised and semi-supervised learning models using mutual information and matrix entropy difference as constraints in the loss function. [Fig.4 a, b, c](#) present the semi-supervised learning performance of some SOTA method, such as FreeMatch²⁷, SoftMatch²⁸ and OTMatch²⁹ and [Fig. 4 d](#) presents performance of supervised with and without max MI and min HD. It is observed that applying maximizing matrix mutual information and minimizing matrix entropy difference led to a slight improvement in supervised learning performance. We believe this is because sufficient labeled data provides adequate information constraints, leading to only a modest enhancement in performance. However, in semi-supervised learning, in most settings, maximizing matrix mutual information and minimizing matrix entropy resulted in the best or second-best performance. Additionally, our method consistently outperformed our baseline, FreeMatch²⁷, across various settings. This suggests that in situations with insufficient labeled samples, additional information constraints can more effectively improve model performance.

Discussion

We introduce matrix information theory as an analytical tool to analyze the training process of supervised learning. Experiments show that merely observing whether the matrix entropy of sample representations or classification head weights reaches the theoretical value of Neural Collapse is insufficient to accurately determine if the model has reached the state of Neural Collapse. We also find that for a set of representation, the lower the matrix information entropy, the better the clustering of these representations. Based on the properties of matrix information entropy, we propose a new cross-modal alignment (CMA) loss. We optimize the fine-tuning process of cross-modal pre-trained models by minimizing the matrix information entropy of representations from different modalities of the same category. CMA can effectively enhance the cross-modal alignment capability of pre-trained models and improve their performance.

In addition, we have made significant advancements in understanding the dynamics of supervised learning by utilizing matrix information and Neural Collapse theory. In order to describe Neural Collapse accurately, we propose two new metrics: the matrix mutual information rate and the matrix entropy difference rate. Our introduction of matrix mutual information ratio (MIR) and matrix entropy difference ratio (HDR) provide novel insights into the interplay between data representations and classification head vectors, serving as new tools to understand the dynamics of neural networks. Through a series of rigorous theoretical and empirical analyses, we demonstrate the effectiveness of MIR and HDR in elucidating various neural network

phenomena, such as linear mode connectivity and grokking. The incorporation of these metrics as loss functions in supervised and semi-supervised learning shows promising results, indicating their potential to enhance model performance and training efficiency. This study not only contributes to the field of machine learning by offering new analytical tools but also applies matrix information to optimize supervised learning.

Method

Pipeline of supervised learning and semi-supervised learning

In supervised learning, we train the neural network h and classifier $W \in \mathbb{R}^{c \times d}$ on the dataset $\mathcal{D}_L = \{(x_i, \sim y_i)\}_{i=0}^{N_L}$ consisting of N_L samples. h is used to extract data features $f \in \mathbb{R}^D$, and W classifies the extracted features. The model is optimized using the following cross-entropy loss.

$$\mathcal{L}_s = \frac{1}{B} \sum_{i=1}^B \mathcal{H}(y_i, p(\omega(x_i))),$$

where B represents the batch size, \mathcal{H} denotes the cross-entropy loss, $p(\cdot)$ refers to the model's output probability of a sample, and ω means random data augmentation.

Compared to supervised learning, semi-supervised learning includes an additional unlabeled dataset $\mathcal{D}_u = \{u_i\}_{i=0}^{N_U}$ which contain N_U unlabeled data and utilizes it to assist in optimizing the model. In the processing of unlabeled data, we adopt the approach outlined in Freematch²⁷. This involves generating pseudo-labels through weak data augmentation and selecting data based on a probability threshold. The model is then employed to extract features from strongly augmented data for the computation of cross-entropy loss in conjunction with the pseudo-labels. The formulaic representation of the training objective for unlabeled data is as follows:

$$\mathcal{L}_u = \frac{1}{\mu B} \sum_{i=1}^{\mu B} \mathbb{I}(\max(q_i) > \tau) \cdot \mathcal{H}(\hat{q}_i, Q_i),$$

where q_i and Q_i correspond to $p(y|\omega(u_i))$ and $p(y|\Omega(u_i))$, respectively. The term \hat{q}_i refers to one-hot pseudo-labels generated from q_i . The symbol $\mathbb{I}(> \tau)$ denotes the indicator function applied to values surpassing the threshold τ .

Furthermore, ω and Ω are used to distinguish between weak and strong data augmentation.

The overall optimization objective is

$$\mathcal{L}_{ssl} = \mathcal{L}_s + \lambda \mathcal{L}_u,$$

Where λ represents the weight of \mathcal{L}_u .

Applying information interplay in supervised learning and semi-supervised learning

In a batch of labeled data $\{(x_i, y_i)\}_{i=1}^B \in \mathcal{D}_L$, h extracts feature representations, denoted as $f \in \mathbb{R}^{B \times D}$. In Neural Collapse, the representation of each sample's class center aligns with the classifier weight of the respective category, i.e., $V =$

$[W_{y_1} \cdots W_{y_B}] \in \mathbb{R}^{B \times d}$. In the case of unlabeled data $\{u_i\}_{i=1}^{\mu B} \in \mathcal{D}_U$, we select sample features f' from μB samples with pseudo-label probabilities greater than τ . i.e.,

$f' = \{f_i \in f \mid I(\max(q_j)) > \tau\}$, and obtain the corresponding class centers $V' =$

$[W_{y'_1} \cdots W_{y'_{\mu B}}] \in \mathbb{R}^{\mu B \times d}$, where y'_i is the pseudo label of f'_i .

Maximizing mutual information. We add an additional loss term to increase the mutual information between them. For supervised learning, the final optimization objective is

$$\mathcal{L} = \mathcal{L}_s - \lambda_{mi} \cdot \text{MI}(G(f), G(V)).$$

For semi-supervised learning, the final optimization objective is

$$\mathcal{L} = \mathcal{L}_{ssl} - \lambda_{mi} \cdot \text{MI}(G(f'), G(V')),$$

where λ_{mi} is the weight for the mutual information.

Minimizing entropy difference. In supervised learning, the ultimate optimization target is delineated as

$$\mathcal{L} = \mathcal{L}_s + \lambda_{id} \cdot |\text{H}(G(f)) - \text{H}(G(V))|.$$

Regarding semi-supervised learning, this target shifts to

$$\mathcal{L} = \mathcal{L}_{ssl} + \lambda_{id} \cdot |\text{H}(G(f')) - \text{H}(G(V'))|,$$

wherein λ_{id} signifies the weight for entropy difference.

Pipeline of cross-modal few-shot fine-tuning

In cross-modal few-shot fine-tuning, we utilize a few-shot dataset $\mathcal{D} \subset \mathcal{X} \times \mathcal{Y}$, where each image $x \in \mathcal{X}$ is paired with its corresponding label name $y \in \mathcal{Y}$. This dataset \mathcal{D} is used to fine-tune the cross-modal pre-trained model, which comprises an image encoder f_θ and a corresponding text encoder g_θ . We set the weights of the classifier using the text encoder as $\{W_i\}_{i=1}^C = g_\theta([P, y_i])$, where P represents the prompts token and C is the number of classes. Then we calculate the feature of each image $f_\theta(x)$ and the predication probability is

$$p(y = i|x) = \frac{\exp(\cos(W_i, f_\theta(x)))}{\sum_{j=1}^C \exp(\cos(W_j, f_\theta(x)))}.$$

The model is optimized by cross-entropy loss:

$$\mathcal{L}_{ce} = \frac{1}{B} \sum_{i=1}^B \mathcal{H}(y_i, p(x_i)),$$

where B represents the batch size. \mathcal{H} denotes the cross-entropy loss, $p(x_i)$ refers the model's output probability of x_i . The essence of cross-modal pre-training fine-tuning is to align the features of different modalities.

Applying CMA into few-shot fine-tuning

We propose to using representations from various modalities to construct a cross-modal Gram matrix. Specially, for each class, we collect the representations of image and text, i.e., $F_c = \{f_\theta(x_i), g_\theta([P, y_i])\}$, where $y_i = c$. The cross-modal alignment loss (CMA) is as follows:

$$\mathcal{L}_{cma} = \sum_{i=0}^c H(G(F_i)).$$

The final optimization objective is

$$\mathcal{L} = (1 - \lambda) \cdot \mathcal{L}_{ce} + \lambda \cdot \mathcal{L}_{cma},$$

where λ is the weight of cross-modal alignment loss.

Experiment details

Supervised learning and semi-supervised learning. In our effort to conduct a fair comparison between our proposed method and existing methodologies, we meticulously designed our experiments building upon previous scholarly work. TorchSSL³⁰, a sophisticated codebase encompassing a wide array of semi-supervised learning techniques as well as supervised learning implementations, is employed as our foundational codebase. TorchSSL enables us to implement our algorithm effectively and assess its performance on well-established datasets like CIFAR-10, CIFAR-100, and STL-10. In the realm of supervised learning, our unique loss components are applied to annotated data, facilitating the computation of both mutual information loss and information entropy difference loss. For semi-supervised learning scenarios, these loss components are extended to unlabeled data, enhancing the calculation of these loss metrics during the unsupervised learning phase. We use an SGD optimizer, configured with a momentum of 0.9 and a weight decay parameter of $5e^{-4}$. The learning rate was initially set at 0.03, subject to cosine annealing. We report the performance metrics over several runs of seeds. The batch size are maintained at 64 across a comprehensive 1,048,000 iterations training regimen. Concerning model architecture, WideResNet-28-2, WideResNet-28-8, and WideResNet-37-2 are respectively chosen for datasets CIFAR-10, CIFAR-100, and STL-10.

Few-shot fine-tuning. In few-shot fine-tuning, we follow CoOp and CoCoOp for a fair comparison. we use open source ResNet-50 and ViT-B/16 as the backbone of the CLIP, and evaluate our method on 11 different datasets, which contain ImageNet,

StanfordCars, UCF101, Caltech101, OxfordFlowers, SUN397, DTD, EuroSAT, FGVC Aircraft, OxfordPets and Food101. These datasets cover a wide range of different visual recognition tasks such as generic object classification, fine-grained classification, action, scene, texture, etc.

Data availability

All datasets used in this paper are available in the open-source repository^{1,14–23,31,32}.

Code availability

Our code is based on CoOp¹³ and TorchSSL³⁰. Our code can be available at <https://github.com/skingorz/CMA>.

Reference

- 1 Krizhevsky A, Sutskever I, Hinton GE. Imagenet classification with deep convolutional neural networks. In: *Advances in neural information processing systems*. 2012, pp 1097–1105.
- 2 Lin T-Y, Maire M, Belongie S, Hays J, Perona P, Ramanan D *et al*. Microsoft coco: Common objects in context. In: *European conference on computer vision*. Springer, 2014, pp 740–755.
- 3 Pappayan V, Han X, Donoho DL. Prevalence of neural collapse during the terminal phase of deep learning training. *Proc Natl Acad Sci* 2020; **117**: 24652–24663.
- 4 Frankle J, Dziugaite GK, Roy D, Carbin M. Linear mode connectivity and the lottery ticket hypothesis. In: *International Conference on Machine Learning*. PMLR, 2020, pp 3259–3269.
- 5 Power A, Burda Y, Edwards H, Babuschkin I, Misra V. Grokking: Generalization beyond overfitting on small algorithmic datasets. *ArXiv Prepr ArXiv220102177* 2022.
- 6 Song K, Tan Z, Zou B, Ma H, Huang W. Unveiling the Dynamics of Information Interplay in Supervised Learning. In: *Forty-first International Conference on Machine Learning*. PMLR, 2024.
- 7 Skean O, Osorio JKH, Brockmeier AJ, Giraldo LGS. DiME: Maximizing Mutual Information by a Difference of Matrix-Based Entropies. *ArXiv Prepr ArXiv230108164* 2023.
- 8 Roy O, Vetterli M. The effective rank: A measure of effective dimensionality. In: *European Signal Processing Conference*. IEEE, 2007, pp 606–610.
- 9 Zhang Y, Tan Z, Yang J, Huang W, Yuan Y. Matrix Information Theory for Self-Supervised Learning. *ArXiv Prepr ArXiv230517326* 2023.
- 10 Rousseeuw PJ. Silhouettes: a graphical aid to the interpretation and validation of cluster analysis. *J Comput Appl Math* 1987; **20**: 53–65.
- 11 Davies DL, Bouldin DW. A cluster separation measure. *IEEE Trans Pattern Anal Mach Intell* 1979; **PAMI-1**: 224–227.
- 12 Radford A, Kim JW, Hallacy C, Ramesh A, Goh G, Agarwal S *et al*. Learning transferable visual models from natural language supervision. In: *International Conference on Machine Learning*. PMLR, 2021, pp 8748–8763.

- 13 Zhou K, Yang J, Loy CC, Liu Z. Learning to Prompt for Vision-Language Models. *Int J Comput Vis* 2022; **130**: 2337–2348.
- 14 Fei-Fei L, Fergus R, Perona P. Learning generative visual models from few training examples: An incremental bayesian approach tested on 101 object categories. In: *Computer Vision and Pattern Recognition Workshop*. IEEE, 2004.
- 15 Cimpoi M, Maji S, Kokkinos I, Mohamed S, Vedaldi A. Describing textures in the wild. In: *Proceedings of the IEEE Conference on Computer Vision and Pattern Recognition*. 2014, pp 3606–3613.
- 16 Helber P, Bischke B, Dengel A, Borth D. Eurosat: A novel dataset and deep learning benchmark for land use and land cover classification. *IEEE J Sel Top Appl Earth Obs Remote Sens* 2019; **12**.
- 17 Maji S, Rahtu E, Kannala J, Blaschko M, Vedaldi A. Fine-grained visual classification of aircraft. *ArXiv Prepr ArXiv13065151* 2013.
- 18 Bossard L, Guillaumin M, Van Gool L. Food-101—mining discriminative components with random forests. In: *European Conference on Computer Vision*. Springer, 2014.
- 19 Nilsback M-E, Zisserman A. Automated flower classification over a large number of classes. In: *Indian Conference on Computer Vision, Graphics & Image Processing*. IEEE, 2008.
- 20 Parkhi OM, Vedaldi A, Zisserman A, Jawahar C. Cats and dogs. In: *IEEE Conference on Computer Vision and Pattern Recognition*. IEEE, 2012, pp 3498–3505.
- 21 Krause J, Stark M, Deng J, Fei-Fei L. 3d object representations for fine-grained categorization. In: *IEEE International Conference on Computer Vision Workshops*. 2013, pp 554–561.
- 22 Xiao J, Hays J, Ehinger KA, Oliva A, Torralba A. Sun database: Large-scale scene recognition from abbey to zoo. In: *IEEE Computer Society Conference on Computer Vision and Pattern Recognition*. IEEE, 2010.
- 23 Soomro K, Zamir AR, Shah M. UCF101: A dataset of 101 human actions classes from videos in the wild. *ArXiv Prepr ArXiv12120402* 2012.
- 24 Zhou K, Yang J, Loy CC, Liu Z. Conditional prompt learning for vision-language models. In: *Proceedings of the IEEE/CVF Conference on Computer Vision and Pattern Recognition*. 2022, pp 16816–16825.
- 25 Nanda N, Chan L, Lieberum T, Smith J, Steinhardt J. Progress measures for grokking via mechanistic interpretability. In: *International Conference on Learning Representations*. 2022.
- 26 Altıntaş GS, Bachmann G, Noci L, Hofmann T. Disentangling Linear Mode Connectivity. In: *UniReps: the First Workshop on Unifying Representations in Neural Models*. 2023.
- 27 Wang Y, Chen H, Heng Q, Hou W, Fan Y, Wu Z *et al*. FreeMatch: Self-adaptive Thresholding for Semi-supervised Learning. In: *International Conference on Learning Representations*. 2023.

- 28 Chen H, Tao R, Fan Y, Wang Y, Wang J, Schiele B *et al.* SoftMatch: Addressing the Quantity-Quality Trade-off in Semi-supervised Learning. In: *International Conference on Learning Representations*. 2023.
- 29 Tan Z, Zheng K, Huang W. OTMatch: Improving Semi-Supervised Learning with Optimal Transport. In: *International Conference on Machine Learning*. 2024.
- 30 Zhang B, Wang Y, Hou W, Wu H, Wang J, Okumura M *et al.* Flexmatch: Boosting semi-supervised learning with curriculum pseudo labeling. *Adv Neural Inf Process Syst* 2021; **34**: 18408–18419.
- 31 Krizhevsky A, Hinton G, others. Learning multiple layers of features from tiny images. *Citeseer* 2009.
- 32 Coates A, Ng A, Lee H. An analysis of single-layer networks in unsupervised feature learning. In: *Proceedings of the fourteenth international conference on artificial intelligence and statistics*. JMLR Workshop and Conference Proceedings, 2011, pp 215–223.

Acknowledgements

H.M., J.C. and B.Z. are supported by the National Science and Technology Major Project (2022ZD0117902, 2022ZD0117901) and the National Nature Science Foundation of China (No. 62227801, No. U20B2062, No. 62376024, No. 62206015).

Weiran Huang is funded by National Natural Science Foundation of China (62406192), MSR Asia StarTrack Scholars Program, Tencent WeChat Rhino-Bird Focused Research Program, and Doubao LLM Fund.

Author contributions

K.S., Z.T., H.M. and W.H. conceived the research and designed the experiments. Z.T. provided the theoretical results and completed the theoretical proof. K.S. and J.C. performed the experiments of Matrix Entropy and cross-modal alignment loss. K.S., Z.T. and B.Z performed the experiments of information interplay and supervised learning and semi-supervised learning. All authors analyzed the results and wrote the paper.

Competing interests

The authors declare no competing interests.